Multifunctional Carbon for Electrochemical Double-Layer Capacitors

*Birhanu Desalegn Assresahegn and Daniel Bélanger**

Multifunctional carbon materials are prepared for application as an active electrode material in an electrochemical capacitor displaying both charge storage and binder properties. The synthesis of the materials involves the functionalization of high surface area Black Pearls 2000 carbon black by a covalent attachment of polyacrylic acid. The polyacrylic acid polymer is formed by atom transfer radical polymerization using 1-(bromoethyl) benzene groups initially bonded to the carbon by spontaneous grafting from the corresponding diazonium ions. The grafting of 1-(bromoethyl)benzene and polyacrylic acid is confirmed by thermogravimetric analysis, Fourier transform infrared spectroscopy, energy-dispersive X-ray spectroscopy, and nitrogen gas adsorption isotherm. The composite electrode films prepared from the modified carbon are more hydrophilic and have better wettability in an aqueous electrolyte than the one prepared with the unmodified carbon. The modified electrodes also show a higher specific capacitance (≈140 F g^{-1}), a wider working potential window (1.5 V) and excellent specific capacitance retention upon cycling (99.9% after 5000 cycles) in an aqueous 0.65 M K_2SO_4 electrolyte. Moreover, a relatively high specific capacitance (≈90 F g^{-1}) is maintained at a scan rate of 1000 mV s^{-1} with the polyacrylic-acid-modified carbon electrode.

1. Introduction

Currently, there is a worldwide interest in the development of high-performance energy storage systems such as batteries and electrochemical capacitors.[1–5] This is due to their technological importance and use in electronic devices and for the electrification of transportation.[1,6–11] A key constituent of electrochemical capacitors and batteries is the composite electrode (anode and cathode), which commonly consists of an electroactive material, a carbon additive, and a binder. These components are mixed to form a paste and eventually the composite film electrode (**Scheme 1**a). Each component has an important and specific role; the electroactive material provides charge storage properties, the carbon additive contributes to increase the conductivity of the usually low-conductivity electroactive material and the binder ensures the integrity of the composite electrode. A minimum amount of the carbon additive and the binder should be used to avoid a detrimental decrease in energy density of the energy storage system. In practice, the fabrication of a composite electrode requires an optimization of the composition of each component. Approaches to facilitate the electrode fabrication are currently developed and include the elaboration of "binderless" electrode that involves the deposition of a thin film of the active electrode directly on a high-surface area current collector.[12] In spite of this, most of the current industrial electrode materials are based on a composite such as described above.

Traditionally, a strong emphasis has been put on the development and optimization of the active material to enhance the electrochemical performance of energy storage devices,[13–15] while less attention was devoted to the electrochemically inactive components of the composite electrodes, such as the binder.[16] Nonetheless, recent studies have shown that many important characteristics of a composite electrode, such as the stability and rate performance, are critically dependent on the formulation of the electrode and the binder's properties.[16–31] The chemical compatibility of the binder towards the solvents used to prepare the composite electrode is also a very important aspect to consider. Accordingly, there is a strong will to replace organic solvents by water processable materials.[32,33] Binders that have been commonly used to elaborate composite electrodes include hydrophobic polymers such as poly(tetrafluoroethylene) (PTFE) and poly(vinylidene fluoride) (PVDF)[16,19,27,34–36] as well as hydrophilic materials such as sodium salt of carboxymethyl cellulose (CMC) and polyacrylic acid (PAA).[16–24,28] Interestingly, the latter two allow processing of electrodes with water rather than volatile organic solvents. PAA has recently received large attention because it provides a high concentration of carboxylic acid functional groups that gives superabsorbent properties and good wettability for the electrodes in protic electrolytes. It also imparts an ionized surface in water and variety of organic solvents that can facilitate the transport of ions from the electrolyte.[32,33,37–41] Accordingly, PAA has been used with MnO_2 for electrochemical capacitor application[42] and also for Li-ion battery cathode[14,30,40,43–45] and anode.[32,33,37–39,46,47] In these cases, improved performance in terms of energy and power density as well as cyclability has been reported, using aqueous as well as organic electrolytes.

B. D. Assresahegn, Prof. D. Bélanger
Département de Chimie
Université du Québec à Montréal
Case Postale 8888
succursale Centre-Ville
Montréal, Québec H3C 3P8, Canada
E-mail: belanger.daniel@uqam.ca

DOI: 10.1002/adfm.201503738

In this work, we report an innovative approach to prepare an electrode material for electrochemical double-layer capacitor application by chemically grafting a PAA layer, which displays "binder"-like properties, directly onto the surface of a highly porous carbon material. Thus, the resulting material has both charge storage and binder properties. To demonstrate the proof of concept only an active electrode material was used without the conductive carbon additive (Scheme 1b).

The modified carbon was prepared in a two-step process, which consists in the covalent binding of a thin polymerization initiator layer by the diazonium chemistry (Scheme S1, Supporting Information)[48–54] and further addition of PAA on this grafted layer following the well-established atom transfer radical polymerization (ATRP) procedure (Scheme S2, Supporting Information).[52,55–59] The resulting modified carbons were characterized by thermogravimetric analysis (TGA), Fourier transform infrared spectroscopy, energy-dispersive X-ray spectroscopy, and nitrogen gas adsorption isotherms. Finally, composite film electrodes were prepared with these modified carbons and characterized by contact angle measurement, nitrogen gas adsorption isotherms, electronic conductivity measurements, and electrochemistry.

2. Results and Discussion

2.1. Thermal Analysis

The different materials synthesized in this work were characterized by TGA. **Figure 1**a shows the TGA curves for the pristine Black Pearls (BP) carbon, 1-(bromoethyl)benzene-modified BP (BP-A_1), polyacrylic-acid-grafted BP (BP-A_1 -PAA) powders as well as for pristine PAA (inset). For the unmodified BP carbon, no significant weight change was observed between room temperature and 800 °C when the experiment was performed under helium. On the other hand, the BP-A_1 showed a weight loss of about 1.5 ± 0.8 wt% with an onset temperature of 200 °C that is attributed to the departure of the grafted 1-(bromoethyl)benzene groups. The BP-A_1 -PAA showed an onset of weight loss at 300 °C that accounts to 5.5 ± 0.5 wt% and associated with the departure of the chemically grafted species. The observation of an onset of mass loss at a significantly higher temperature than the pristine PAA supports the covalent attachment of the polymer. The chemical grafting of PAA was also investigated by varying the amount of the starting amine molecule and the *tert*-butyl acrylate monomer. Figure 1b shows an exponential increase of the loading of the initiator molecule A_1 (from 1.5 ± 0.8 to 20.1 ± 3.1 wt%) for a fivefold increase of the amount of the amine molecule and the monomer (see also Section 4, Supporting Information).

The theoretical maximum surface coverage of 1-(bromoethyl) benzene molecules to form a monolayer on BP is estimated to 6.64×10^{-10} mol cm^{-2} by assuming that all molecules are in parallel orientation with the substrate (see also Section 5, Supporting Information). Considering a specific surface area of 1500 m^2 g^{-1}, the theoretical loading is expected to be 9.96 mmol g^{-1} for monolayer coverage.[60,61] In our case, the highest loading of the grafted 1-(bromoethyl)benzene groups is ≈10.9 mmol g^{-1} (Table S3, Supporting Information) and represents a surface concentration of 4.4×10^{13} molecules cm^{-2}. Since it is unlikely that all the pores contributing to the total surface area of BP are accessible to the covalent grafting of 1-(bromoethyl)benzene groups,[60] the reported values above can be considered as a lower limit. Thus, the material with the highest loading will consist of multilayers of 1-(bromoethyl)benzene groups as is the case for the spontaneous covalent grafting of different organic molecules by the diazonium chemistry.[60,61]

Another interesting fact observed from the thermal analysis is that when these BP-A_1 powders are subsequently modified by ATRP, it can be seen that the total loading of PAA on the carbon powder surface can be controlled by changing the reaction conditions and reach up to 45.0 ± 0.5 wt%, as shown in Figure 1b. The TGA curves for all the different modified carbons are presented in Figure S1 and S2 (Supporting Information).

2.2. FTIR Characterization

The surface functional groups present on the carbon before and after grafting were investigated by FTIR spectroscopy and representative spectra are shown in **Figure 2**. Figure 2a shows

Birhanu D. Assresahegn is currently a Ph.D. student at the Département de Chimie, Université du Québec à Montréal, Canada. He received a joint M.Sc. Degree in Materials for Energy Storage and Conversion from Université Paul Sabatier Toulouse III, France; Université de Picardie Jules Verne, France and Warsaw University of Technology, Poland. His research focuses on surface chemistry and development of new materials for energy storage applications such as electrochemical capacitors and lithium-ion batteries.

Daniel Bélanger is a professor in the Département de Chimie from l'Université du Québec à Montréal. He received his Ph.D. in Energy Sciences from the Institut National de la Recherche Scientifique of the Université du Québec (Canada) in 1985. His research focuses on chemical modification of surfaces, developing new materials for energy storage (e.g. electrochemical capacitors and batteries) applications.

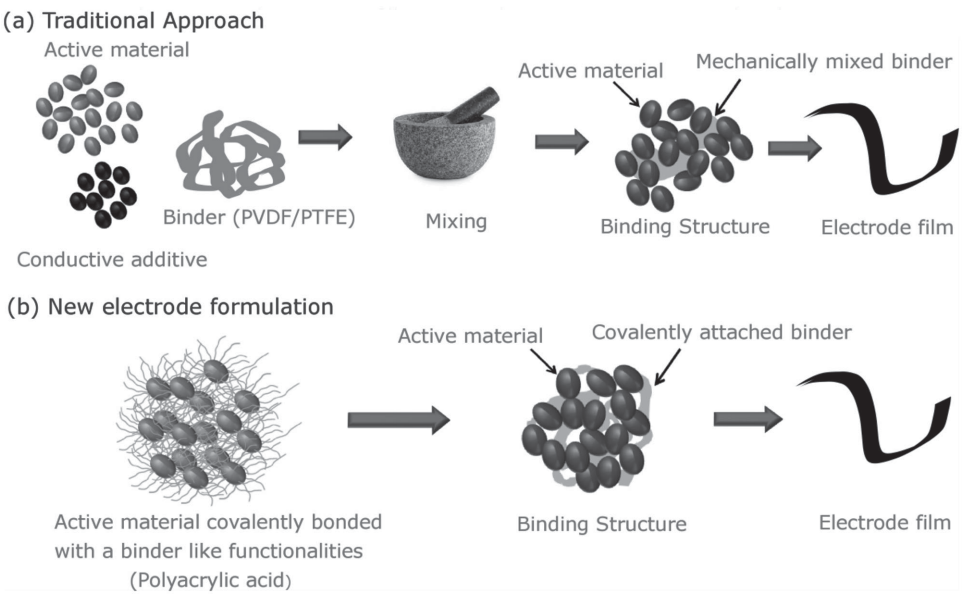

Scheme 1. Schematic representation of the: a) traditional approach for the fabrication of a composite electrode and b) the new electrode formulation based on bifunctional materials.

a wide IR absorption band centered at around 1080 cm^{-1} that is associated mainly with the C–H vibration of the BP carbon.[62] The band is also observed for both BP-A_1 and BP-A_1-PAA centered at the same frequency, although its shape and width are different, (Figure 2b,c, respectively). This is consistent with the grafting of the surface ATRP initiator (e.g., 1-(bromoethyl)benzene). This particular absorption band does not provide much information by itself. More compelling evidence for the grafting of 1-(bromoethyl)benzene is demonstrated by the presence of the benzene (C=C) vibration bands at 1560 and 1620 cm^{-1} and the bands at 2840 and 2930 cm^{-1} due to the C–H stretching vibration of the alkyl groups of the initiator and polymer chain. Interestingly, the spectrum of BP-A_1 does not show the characteristic sharp band at 2258 cm^{-1} for the N_2^+ group, which is a good indication that the A_1 diazonium ions have been reduced and the resulting aryl radical is grafted on the carbon powder surface. The BP-A_1-PAA spectra (Figure 2c) contains the major vibration bands observed for the pristine PAA (Figure 2d) such as the C=O stretching vibration at 1720 cm^{-1}, the carboxylic acid C–O stretching vibration at 1245 cm^{-1} and O–H vibration band at around 3250 cm^{-1}, which confirms the presence of PAA on the carbon black powder surface.

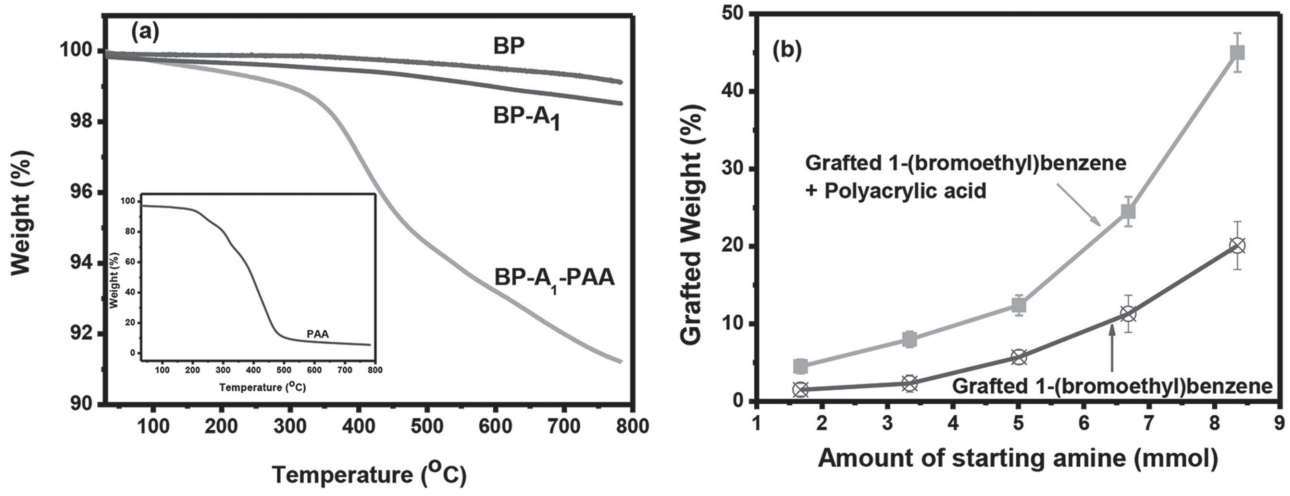

Figure 1. a) TGA profile for the pristine BP carbon, BP-A_1, and BP-A_1-PAA in the temperature range of 30 °C to 800 °C and 5 °C min^{-1} heating rate under helium gas flow (Inset: TGA profile for polyacrylic acid, PAA). b) Variation of the loading of the grafted 1-(bromoethyl)benzene and polyacrylic acid on BP as a function of amount of the starting amine and corresponding monomer (see also Table S2, Supporting Information, for complete experimental conditions of the grafting).

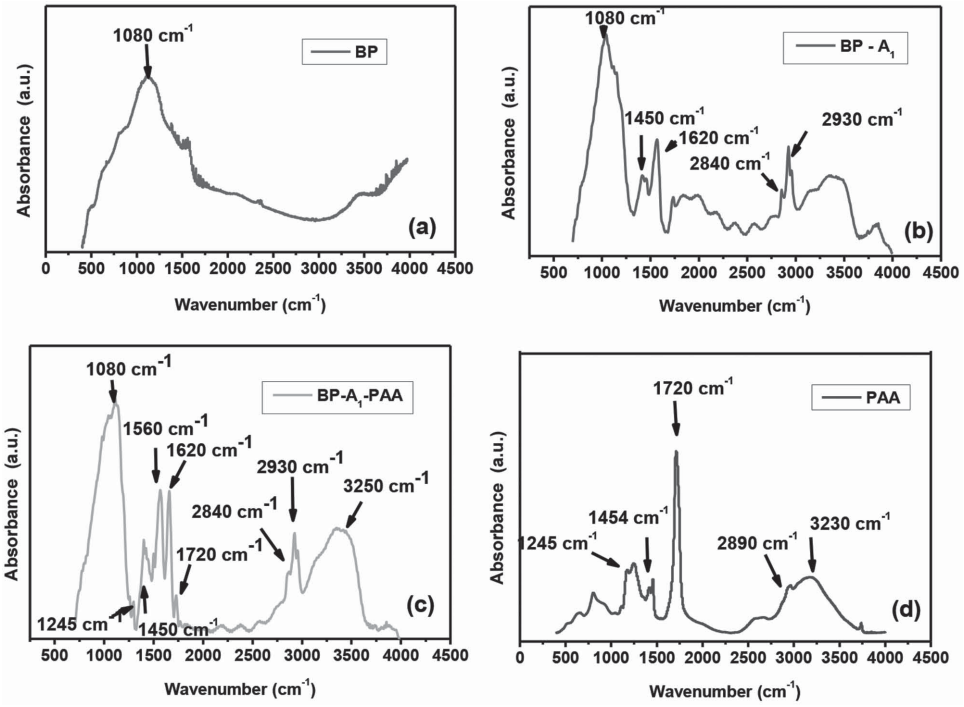

Figure 2. FTIR spectra for: a) unmodified BP; b) BP-A_1 (1.5 wt% grafted); c) BP-A_1-PAA (5 wt% grafted) and d) pristine polyacrylic acid.

2.3. Microstructural and Composition Analysis with Scanning Electron Microscopy and Energy-Dispersive X-ray Spectroscopy

Figure 3 shows SEM images of the pristine and the polyacrylic-acid-grafted BP carbon. The pristine carbon powder showed relatively scattered particles with an approximate average size of about 40 nm (Figure 3a). The characteristic feature that can easily be recognized from the SEM images is the increase in the extent of agglomeration of the carbon particles following modification (Figure 3b). This can be attributed to the high concentration of –COOH functionalities introduced, which results a strong H-bond interaction between them. The polyacrylic-acid-functionalized carbon particles tend to agglomerate and possess a spongy-like morphology unlike the unmodified carbon particles. The grafting of 1.5 wt% of 1-(bromoethyl)benzene groups and 5 wt% of PAA also showed an approximate increase of 0.6 ± 0.1 nm and 2.7 ± 0.3 nm of the particle size, respectively (for the former see Figure S3, Supporting Information).

From the ≈2.1 nm difference in the particle sizes between BP-A_1 and BP-A_1-PAA, the average number of acrylic acid monomer units attached to A_1 can be roughly estimated. Knowing that the average C–C single-bond length is 137 pm,[63] a 2.1 nm thickness represents 15 acrylic acid monomer units. The optimum loading of PAA is unknown at the moment but most likely a bifunctional carbon with a relatively low molecular weight of the grafted PAA is required to fully take advantage of the charge storage properties of the carbon while having a material with sufficient binder-like behavior. From the 2.1 nm thickness of the grafted material, a loading of ≈8.5 wt% can also be roughly estimated, which is reasonably in a good agreement with the value determined by TGA (see also Section 8, Supporting Information, for the calculations).

The EDX spectra shown in Figure 3c,d for both pristine BP carbon and the modified BP-A_1-PAA carbon can also give additional information about the presence of the PAA and (1-(bromoethyl)benzene) functionalities on the carbon surface (for the latter see Figure S4, Supporting Information). For the unmodified BP carbon spectra, the expected strong peak for carbon and a relatively weak peak for oxygen are observed. In the spectra for the modified carbons, in addition to the C and O peaks, the presence of a significant bromine peak is due to the terminal atom in the initiator organic molecule (e.g., 1-(bromoethyl)benzene) and the PAA chains. This further confirms that the initiator grafting and polymerization steps were successful. The bromine content of BP-A_1 and BP-A_1-PAA samples reveals no significant difference.

2.4. Adsorption Isotherms and Porosity Analysis

Nitrogen adsorption isotherms for the unmodified Black Pearls carbon powder and various composite films made with BP following modification by 1-(bromoethyl)benzene and polyacrylic acid surface grafting are shown in **Figure 4**a. The isotherm of the Black Pearls carbon powder shows the adsorption of a large volume at low P/P_0 (e.g., below 0.1), which is characteristic of an extended microporous structure.[61] In contrast, the BP-A_1-PAA samples are characterized by a smaller adsorbed volume in the same P/P_0 range. In the intermediate P/P_0 range, between 1 and 0.8, the slightly sloped plateau

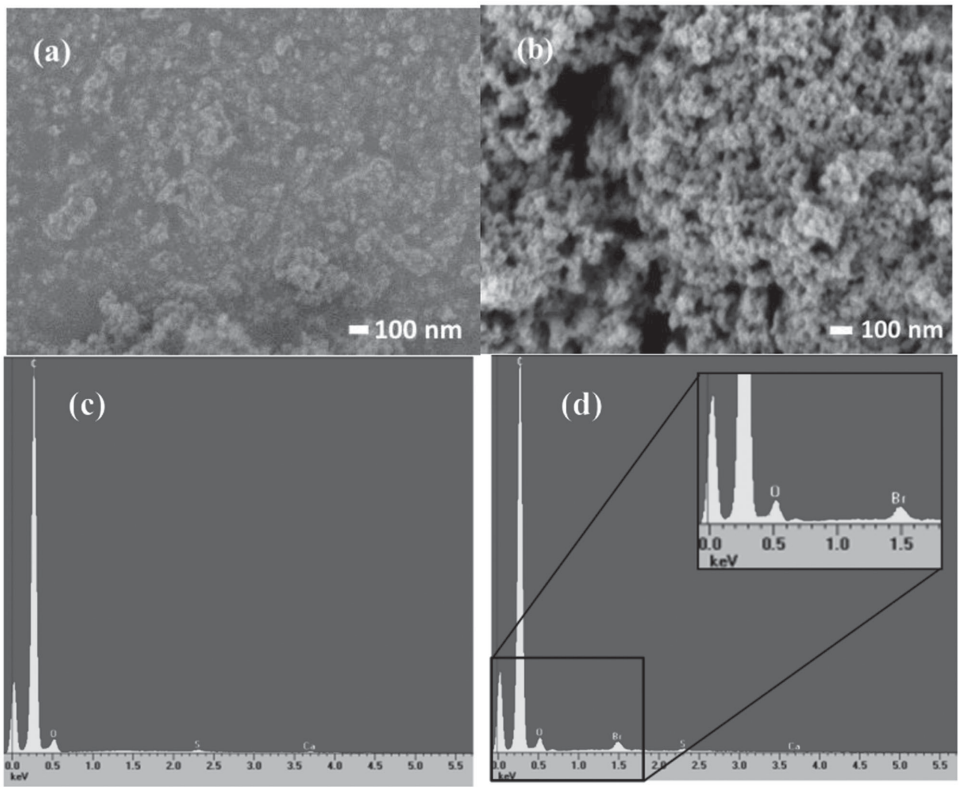

Figure 3. a,b) SEM image with ×45 000 magnification c,d) EDX spectra for pristine BP and BP-A_1-PAA (5 wt% grafted) carbon, respectively.

observed for all the materials is mainly due to a contribution from adsorption in the mesopores.[61] Figure 4b,c show that the pore size distribution and surface area contribution, respectively, for the pristine carbon comes mainly from the micropores (<2 nm) in addition to mesopores (between 2 and 5 nm). However, it is clearly seen that the modification of the carbon completely blocks adsorption of N_2 by the micropores (especially those less than 1.2 nm) unlike the composite films prepared by simple mixture of the carbon and the PTFE binder.

The measured BET surface area (Table S4, Supporting Information) of BP carbon is decreasing from 1500 to 1300 and 950 $m^2\ g^{-1}$ for a composite film containing 10 and 25 wt% of PTFE binder, respectively. The measured value for the former composite film is in good agreement with the expected surface area (90 wt% BP ≈1350 $m^2\ g^{-1}$) if the surface area contributed by the PTFE binder is neglected. However, for the sample containing 25 wt% of PTFE, thus 75 wt% of BP, the expected surface area should be 1125 $m^2\ g^{-1}$. The observation of a lower experimental value of 950 $m^2\ g^{-1}$ suggests that the pore structure is affected [36] while the opposite is true for the addition of a lower fraction of binder. A similar decrease of the BET surface area was found for composites made with pristine PAA mixed with Black Pearls carbon (Table S4, Supporting Information). However, for the composite films made from the PAA-modified carbons, a much higher BET surface area loss of ≈30% and ≈65% is obtained for the 6 and 25 wt% PAA loading, respectively (Table S4, Supporting Information). These results indirectly prove that the synthesized PAA of the chemically modified carbons is not physically adsorbed.

2.5. Contact Angle Measurements

Static contact angle measurements were performed for films prepared with different carbon compositions to determine the change in their surface properties (e.g., hydrophilicity and hydrophobicity) accompanying PAA grafting. **Figure 5** shows images of sessile droplets and the measured contact angle values for various BP-A_1-PAA films and compared to those prepared using a PTFE binder. It can be clearly seen that the grafting of PAA on BP carbon makes it more hydrophilic as demonstrated by the small contact angles measured. Increasing the PAA content makes the modified film more hydrophilic. On the other hand, the addition of PTFE enhances the hydrophobicity of the resulting film. For the electrode film prepared from BP-A_1-PAA with 25 wt% loading of grafted species, the solvent takes less than 30 s to dissipate through the material and an accurate contact angle value cannot be taken (see Figure S5, Supporting Information). This hydrophilic property of the BP-A_1-PAA film could be useful for its application as electrode in aqueous electrolyte-based electrochemical capacitors. Since such a property could provide a superabsorbent, highly wettable and ionized material in protic solvents, it can improve accessibility of the pores and facilitates ion transport

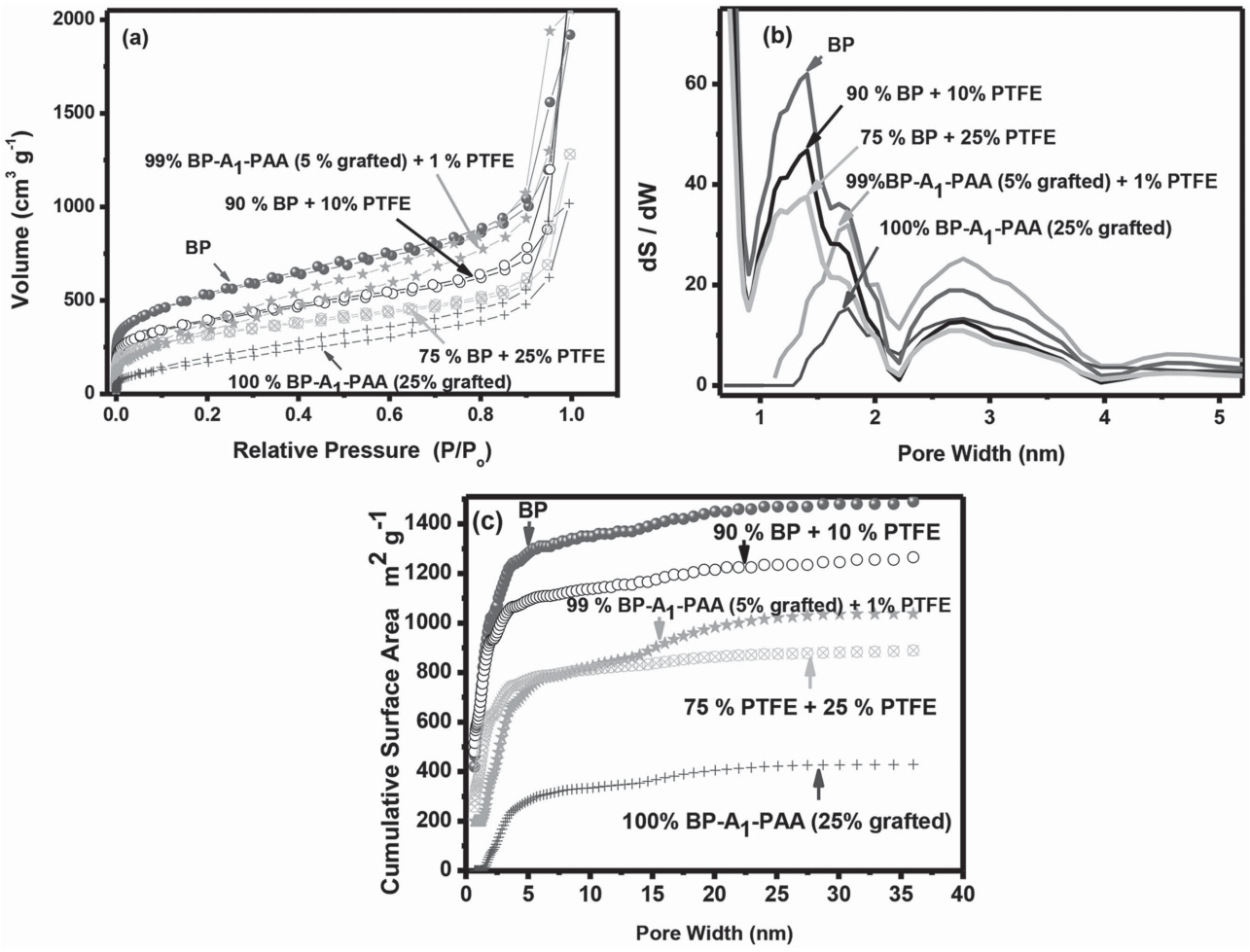

Figure 4. a) Nitrogen adsorption isotherms; b) pore size distribution, and c) cumulated surface area as a function of pore width for the unmodified BP powder and different film compositions.

within the electrode.[42] This could potentially enhance the double-layer charge storage behavior of these materials relative to unmodified carbon-based electrodes.

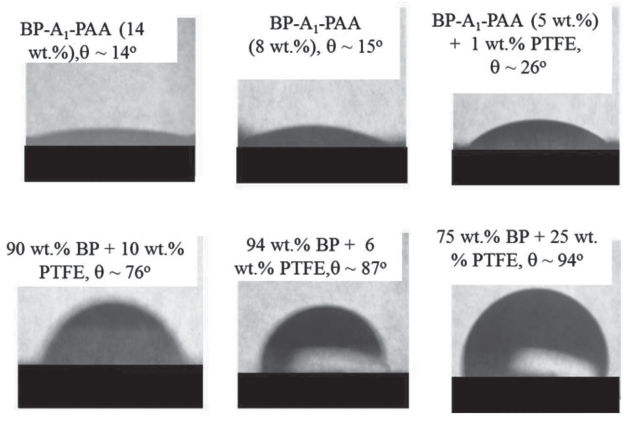

Figure 5. Images of typical sessile droplets for the carbon films of various compositions together with the contact angle.

2.6. Electrochemical Characterization

2.6.1. Composition of the Electrodes

In this work, film electrodes were successfully prepared from the BP-A$_1$-PAA powder with 5 wt% polymer grafting by the addition of only 1 wt% PTFE. This small amount of PTFE is needed to obtain a malleable composite film. Interestingly, a film could be prepared without PTFE and was tested as electrode material but found to be brittle and more susceptible to physical degradation. However, for the carbon powder grafted with higher loading of PAA (e.g., 25 wt%), very good mechanically stable composite films were fabricated without the addition of PTFE. One thing worth noting is that it was not possible to form a composite film by mixing BP with pristine PAA (e.g., without grafting), even by the addition of ≈25 wt%, with the cold-rolling method. Thus, covalent grafting of the PAA appeared to bring good mechanical stability and inter particles adhesion presumably via hydrogen bonding within the PAA chains. Accordingly, several composite film electrodes were prepared with the polyacrylic-acid-grafted BP carbon with and without the PTFE binder and their electrochemical performance were evaluated.

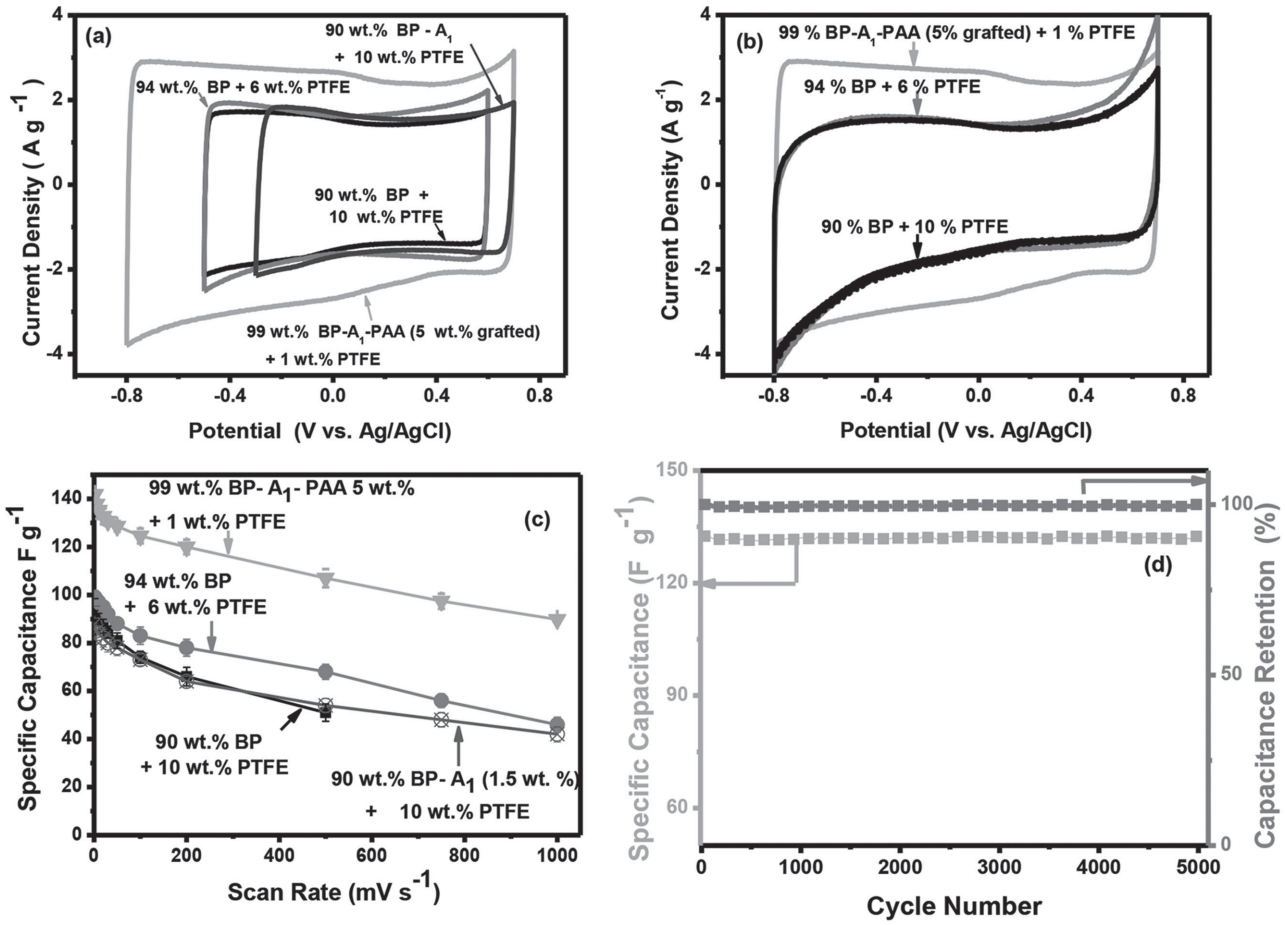

Figure 6. Cyclic voltammograms recorded at 20 mV s^{-1} in aqueous 0.65 M K_2SO_4 electrolyte a) in their respective working potential window and b) in a wider and similar potential window. c) The gravimetric capacitance variation with scan rate for the various composite film electrodes, d) capacity retention for 99% BP-A_1-PAA (5 wt% grafted) + 1 wt% PTFE after 5000 charge/discharge cycles.

2.6.2. Electronic Conductivity of Composite Film Electrodes

Four-point probe measurements made for the different composite films revealed that the modification of the carbon results in only a slight decrease in electronic conductivity of the film (Table S5, Supporting Information). Also, a decrease in electronic conductivity is observed when the loading of the grafted PAA is increased. The small decrease of conductivity following grafting suggests that the formation of defects in the sp^2 regions of the BP powder, due to grafting by the diazonium chemistry,[64] is not too detrimental. Here it is important to notice that the electronic conductivity of the modified material is compared only with a composite film of the same proportion containing the non-conductive PTFE binder, not with the pristine carbon powder.

2.6.3. Electrochemical Properties of the New Materials

The electrochemical properties of the composite film electrodes prepared with the unmodified and modified BP were characterized by cyclic voltammetry. **Figure 6**a shows the cyclic voltammograms in aqueous 0.65 M K_2SO_4 electrolyte solution at a scan rate of 20 mV s^{-1}. All cyclic voltammograms show a rectangular shape that is typical of a capacitive electrode material[65,66] but a significant difference in the working potential window is clearly noticeable. The composite film electrode with the polyacrylic-acid-grafted carbon shows an increase in the working potential range of about 500 mV (see Figure 6a,b). Cyclic voltammograms recorded for the traditional composite film electrodes in the same potential window are characterized by significantly larger parasitic oxidation and reduction current at the positive and negative potential limits, respectively (Figure 6b). This might be attributed to the change in the surface chemistry of the underlying carbon composite electrode upon the covalent attachment of the polyacrylic molecules that would alter the kinetics of the water reduction/oxidation reaction at its surface. Moreover, comparing the shape of the cyclic voltammograms of Figure 6a, when irreversible processes are less important, revealed similar polarization, in agreement with the electronic conductivity measurements. It should be noted that vacuum infiltration has also been utilized to impregnate the pores of the composite electrodes with the electrolyte. In our hands, we found that this procedure does not bring significant improvement in performance compared to the modified electrode material (Figure S6, Supporting Information).

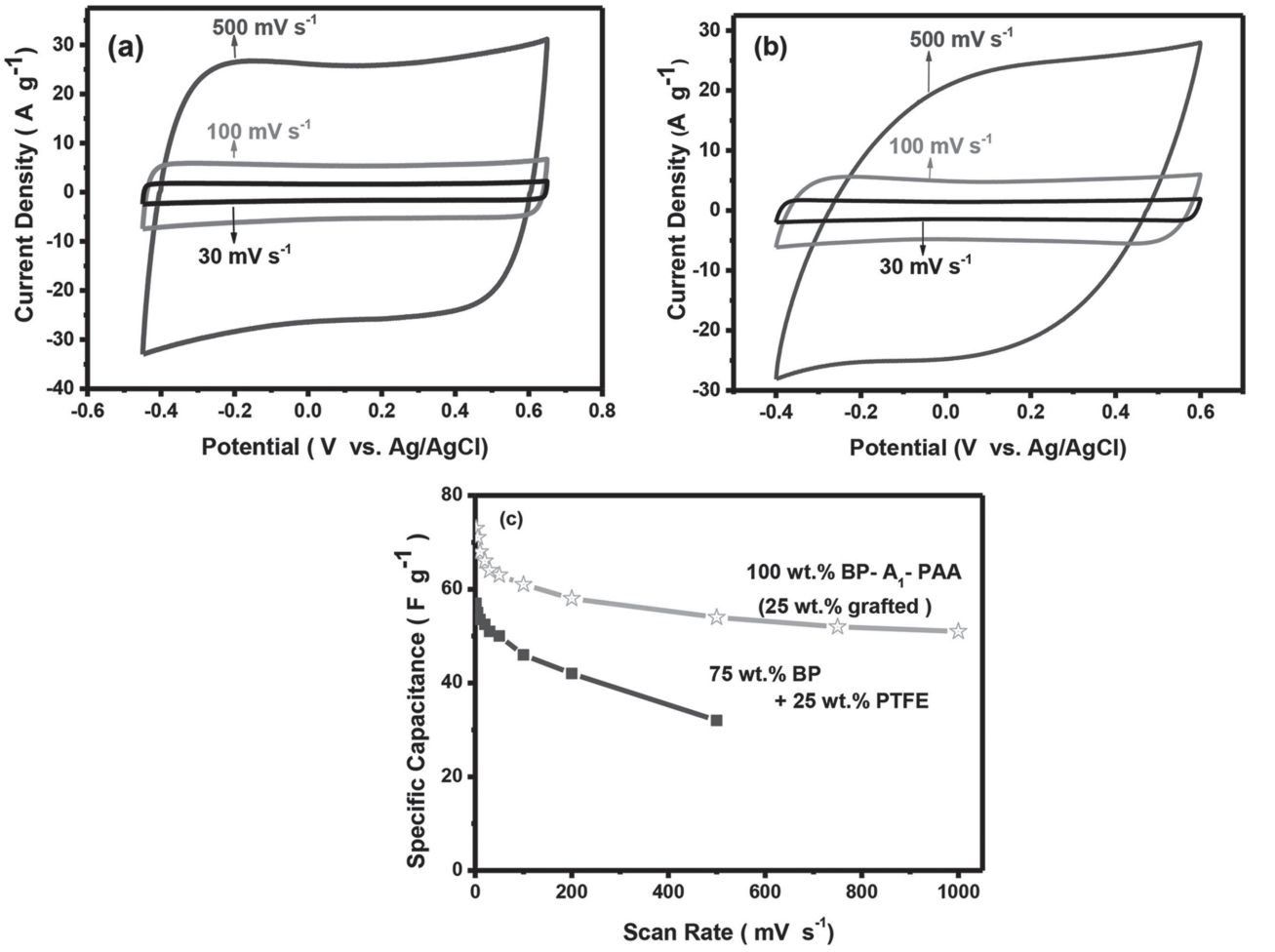

Figure 7. Cyclic voltammograms for a composite electrode fabricated with a) 100% BP-A_1-PAA (25 wt% grafted) and b) 75 wt% BP + 25 wt% PTFE at different scan rates in 0.65 M K_2SO_4 electrolyte, c) Variation of the specific capacitance as a function of scan rate for both electrodes.

The gravimetric and volumetric capacitances of various composite electrodes are also reported in Table S6 (Supporting Information). A 45% improvement of the gravimetric capacitance is noticed for the polyacrylic-acid-grafted BP film electrode. The enhanced performance can be attributed mainly to the presence of the grafted PAA, which possesses a high concentration of surface carboxylic functional groups. These can provide a facilitated transport of ions in the active electrode layer and increase the accessibility of the available pores. Moreover, the increase in capacitance for the electrodes prepared from grafted material might also be partially induced by the grafted PAA groups, which may contribute to the charge storage with their pseudocapacitance. This possibility will be investigated in future studies, for example, by changing the pH of the electrolyte. The good electrochemical performance (both in potential window and capacitance) will enable the composite electrode to provide a high energy and power density for an electrochemical capacitor. Moreover, the similar gravimetric capacitance observed for the composite electrode prepared from the BP carbon onto which only the polymerization initiator is grafted (BP-A_1) with the PTFE binder, clearly shows the contribution of the PAA grafting to the improvement of the gravimetric capacitance. The change in the volumetric capacitance (Table S6, Supporting Information) also follows a trend similar to that of the gravimetric capacity demonstrating that the electrode films are prepared with a uniform density.

Figure 6c also shows the variation of the gravimetric capacitance as a function of the scan rate for various electrodes. It is noteworthy that the BP-A_1-PAA electrode maintained a significantly higher gravimetric capacitance at all scan rates and with a value of about 90 F g^{-1} at 1000 mV s^{-1}. The composite electrodes made with similar proportion of BP carbon and PTFE showed a lower gravimetric capacitance and rapid decline, below 50 F g^{-1}, at a scan rate of 1000 mV s^{-1}. The electrode prepared from the carbon grafted with the polymerization initiator (BP-A_1) only and PTFE binder also delivered a lower gravimetric capacitance compared to BP-A_1-PAA at all scan rates. Furthermore, the long-time cycling stability of the 99% BP-A_1-PAA (5 wt% grafted) + 1 wt% PTFE film electrode is very good with a 99.9% capacity retention after 5000 charge/discharge cycles, as shown in Figure 6d indicating that there is minimal loss in the carbon particle to particle or current collector grid to carbon particle contact.

The electrochemical performance of composite electrodes prepared by using a much higher loading of grafted PAA (25 wt%) without PTFE was also compared to a 75 wt% BP + 25 wt% PTFE electrode. **Figure 7**a demonstrates the superior performance of the BP-A_1-PAA electrode and its ability to maintain a higher specific capacitance, especially at high scan rates (rectangular voltammogram at 500 mV s^{-1}), compared to the electrode made with a PTFE binder of similar proportion (Figure 7b). The observation of much lower polarization for the BP-A_1-PAA electrode is intriguing since both film electrodes have similar electronic conductivity. Figure 7c, shows that a higher specific capacitance at all scan rates is obtained for the 100% BP-A_1-PAA (25 wt% grafted) composite film electrode despite its lower BET surface area (Table S4, Supporting Information). However, the specific capacitance is much lower than the one obtained at the lowest loading of grafted PAA (5 wt%) carbon film electrode, presumably because of the significantly lower surface area of the material.[67]

The overall good electrochemical performance of the new composite electrodes can be mainly attributed to the better wettability of the film made from BP-A_1-PAA compared to the BP + PTFE in aqueous electrolyte. Also, the ionized surface of the BP-A_1-PAA would impart lower ionic resistance.

3. Conclusions

Surface functionalization of Black Pearls carbon by ATRP of PAA was successfully carried out. The new material with functionalization of the carbon surface proved to give a much improved gravimetric/volumetric capacitance and wide working potential window for the resulting composite electrode. The improved performance is related to the presence of ionizable surface carboxylate functional groups, which can provide good electrolyte accessibility to the pores and surface wettability of the active layer, a high ionic conductivity together with a good chemical and mechanical stability in aqueous electrolyte. Even if the covalent linkage of the PAA chains to the BP carbon cannot be directly demonstrated, indirect evidence for grafting is obtained from TGA, gas adsorption measurements, and the ability to form a film (vide supra). One aim of our work was to develop multifunctional materials for energy storage applications. First, a bifunctional material is obtained by grafting a binder to an active carbon powder. Furthermore, other characteristics of electrodes fabricated with these materials such as increased capacitance, wider working potential window, and better wettability insure multifunctional character to these polyacrylic-acid-modified carbons.

In this study, the widely used BP carbon black material in our laboratory was selected to demonstrate the proof of concept that the modification method can be used to functionalize an active material of an energy storage device. In the future, it will also be very interesting to extend our approach to other carbon materials that are commonly used in commercial EDLC.

4. Experimental Section

Chemicals: Black Pearls 2000 carbon black (Cabot), 4-(1-hydroxyethyl)-aniline (Alfa Aesar, 97%), hydrobromic acid (HBr) 48% wt/vol (Aldrich), tetrafluoroboric acid solution (Fisher Scientific, 48%), sodium nitrite, ($NaNO_2$) (NICE, 96%), sodium tetrafluoroborate ($NaBF_4$) (Aldrich), methanol (EMD), *N,N*-dimethyl formamide (DMF) (EMD), acetone (EMD), *tert*-butyl acrylate (*t*-BA) (Aldrich), toluene (EMD), 1-phenylethyl bromide (1-PEBr) (Aldrich), *N,N,N,N′,N′,N″*-pentamethyldiethylenetriamine (PMDETA) (Alfa Aesar), cupric chloride ($CuCl_2$) (Aldrich), cuprous chloride (CuCl) (Aldrich), methylene dichloride (EMD), andtrifluoroacetic acid (CF_3CO_2H) (Alfa Aesar, 99%), and PAA (average M_W = 25 000 g mol^{-1}; Aldrich) were analytical grade and used as received. All solutions and subsequent dilutions were carried out using deionized water (Barnstead Nanopure II).

Synthesis: The ATRP initiator molecule was synthesized by adopting a published procedure[52] described in details in Scheme S1a (Supporting Information). Briefly, the procedure involves the reaction of 4-(1-hydroxyethyl)aniline (1.67 mmol) with HBr 48% (wt/vol) to afford the ATRP initiator molecule, p-(1-bromoethyl)aniline hydrobromide, having a bromine terminal group while keeping the amine group for diazotization.

The diazotization and grafting were done by adding 0.2 g of Black Pearls (BP) carbon to the mixture obtained above with constant stirring for 15 min. Then, the p-(1-bromoethyl)benzene diazonium ions were generated in situ by adding 5 mL HBF_4 and 0.35 mmol of $NaNO_2$, which was accompanied by a nitrogen gas evolution (Scheme S1b, Supporting Information). The reaction was allowed to last overnight with constant stirring of 300 rpm at ambient temperature. Finally, the reaction mixture was vacuum filtered on a Nylon membrane having a pore size diameter of 0.47 µm (Pall) and washed sequentially with 5% (wt/vol) $NaBF_4$ (≈1 L), methanol (≈750 mL), ethyl ether (≈500 mL), and acetone (≈500 mL) to afford the ATRP initiator molecule, 1-(bromoethyl)benzene groups grafted on Black Pearls carbon (BP-A_1) (Scheme S1c, Supporting Information).

The 1-(bromoethyl)benzene molecule grafted on BP contains a very good leaving group (–Br) to initiate ATRP of vinyl monomers, in the presence of proper catalysts. This enables the polymerization to occur on the surface of the modified carbon rather than in the solution. The monomer used to initiate the polymerization was *tert*-butyl acrylate (*t*-BA) since acrylic acid is not readily undergoing surface ATRP.[59] The general procedure is as follows: a 100 mL Schlenck flask reactor equipped with a soccer-ball-shaped magnetic stirrer, a condenser, and nitrogen gas lines were prepared. The catalysts, CuCl and $CuCl_2$ were transferred to the flask and dissolved in 20 mL toluene solvent using a strong sonication for 15 min followed by degassing with nitrogen for 20 min. Thereafter, the BP-A_1 was added and the mixture stirred for a further 10 min. Then, PMDETA, 1-PEBr and *tert*-butyl acrylate (*t*-BA) were sequentially added to the polymerization flask under a nitrogen flow and continuous stirring. Following these additions, the reaction mixture was degassed for 1 h. Then, the flask was kept in an oil bath at 100 °C for 16 h and the polymerization was stopped by cooling and after opening the flask to expose the catalyst to air. Finally, the reaction mixture was filtrated under vacuum on a Nylon membrane and washed sequentially with toluene and acetone in order to remove adsorbed species. This procedure results in the surface grafting of poly (*tert*-butyl acrylate), which can undergo acid hydrolysis to cleave the *tert*-butyl groups and form the desired PAA surface-grafted Black Pearls carbon (BP-A_1-PAA). For this final step, the poly (*tert*-butyl acrylate)-modified carbon was dispersed in 20 mL of methylene dichloride by sonication for 10 min and 25 mL of CF_3CO_2H was slowly added to the above dispersion. After overnight hydrolysis with stirring at room temperature, the BP-A_1-PAA powder was recovered by centrifugation at 4000 rpm for 30 min and the remaining methylene dichloride and excess trifluoroacetic acid were removed by keeping the sample at 80 °C under vacuum for 3 h. The polymerization reaction and details of the proposed reaction mechanisms[52,56,58,59] are summarized in Scheme S2 and S3 (Supporting Information). See also Table S1 and S2 (Supporting Information) for the quantities of each reactant. The variation of the polymer loading on the carbon surface was also investigated by varying the amount of the starting amine molecules from 1.67 up to 8.35 mmol (fivefold) followed by a proportional increment of the *tert*-butyl acrylate monomer concentration while starting with the same amount of carbon (See also Table S2, Supporting Information, for details).

Characterization of the Powders: The thermogravimetric analyses were conducted with a TA Instruments TGA (Q500) equipment. The temperature scan was done between 30 °C and 800 °C at a rate of 5 °C min^{-1} under a 100 mL min^{-1} helium gas flow. Platinum pan sample holders were used for all measurements. Moreover, thermal annealing under inert atmosphere was carried out for the initiator-grafted carbon (BP-A_1) at 150 °C and the polyacrylic-acid-grafted carbon (BP-A_1-PAA) at 250 °C to ensure the removal of physically adsorbed organic molecules and solvents.

Fourier transform infrared (FTIR) spectra were recorded after preparing KBr pellets of the different materials with 1% sample weight composition using a Nicolet 4700 FT-IR (Thermo Electron Cooperation) spectrophotometer. To improve the signal-to-noise ratio, the spectra were recorded by collecting 1000 scans. All spectra were baseline-corrected using OMNIC 6.1 internal software and were unsmoothed.

Microstructural analysis of the powders was carried out by using field-emission gun scanning electron microscopy (FEG-SEM; JEOL/JEM-1230) and electron-dispersive X-ray spectroscopy (EDX) JEOL/JSM840. The particle size distributions of the powders were estimated by measuring the average of 40 particles from each scanning electron microscope images using "image-J" software.

Adsorption isotherms were measured using an Autosorb-1 instrument (Quanta chrome Instrument, USA). The porous texture of the carbons and the different composite films (for those compositions that allow film formation) was characterized using nitrogen as adsorbent at 77 K. The volume of gas adsorbed was recorded for relative pressures ranging from 1×10^{-6} to 1. The N_2 adsorption data were used to calculate the total pore volume and the BET specific surface area (S_{BET}). The pore size distribution cumulated surface and volume histograms were also obtained through simulation of the isotherm by density functional theory (DFT) and Monte-Carlo calculations using the ASW1 software. Since composite films cannot be made by physical mixing of pristine PAA with the BP carbon, the porosity analyses were performed for a sample prepared by dispersing the polymer in ethanol and homogeneously mixing with BP and followed by drying at 105 °C.

Characterization of the Electrodes: Composite electrode films were prepared from different proportions of the BP carbon, BP-A_1, and BP-A_1-PAA using PTFE binder when appropriate. In all cases, the composite powders were mixed in a small volume of ethanol until a homogenized paste-like consistency is obtained and the films were made by cold-rolling. Then, they were placed in a stainless steel grid (80 mesh, 0.127 mm, Alfa Aesar), used as current collector, and pressed for 60 s at 9×10^5 Pa.

Static contact angle measurements for the electrode films were performed at room temperature (before pressing on stainless steel) by the sessile drop method with a water drop of about 5 µL. The measurements were taken 30 s after deposition of the water drop. The "image-J" software was used with a MV-50 camera and a magnification of 6×.

Electrical conductivity measurements for the dried composite electrodes were made by four-point probe measurements using a Keithley 6220 DC precision current source (US). The I–V DC potential sweeps were measured at 100 mV s^{-1} and yielded a linear I–V response. The electronic conductivity of the composite film was obtained, using the resistance determined from the inverse slope of the I–V curve and the thickness of the film.

Electrochemical measurements were performed with a three-electrode configuration in one-compartment cell containing a Ag/AgCl/Cl^-(saturated KCl) reference electrode, a high surface area platinum gauze as a counter electrode, and the carbon film as a working electrode. A de-aerated aqueous 0.65 M K_2SO_4 solution was used as electrolyte and all experiments were performed at room temperature. The reference electrode was kept at about 5 mm of the working electrode during measurements. Moreover, prior to any measurement, the working electrode was dipped in the electrolyte for 20 min to allow the electrolyte to impregnate the electrode porosity.

Cyclic voltammetry (CV) was recorded using a Solartron 1255 FRA potentiostat connected to a PC and the electrochemical setups were controlled with DC Corrware software (Scribner Associates, version 2.8d). The specific capacitance, C_s, expressed in farads per gram (F g^{-1}) of carbon paste was determined from the cyclic voltammogram according to Equation (1):

$$C_s = \frac{\Delta Q}{\Delta E.m} \quad (1)$$

where ΔQ is the voltammetric charge (Coulomb), ΔE is the working potential window (Volt), and m is the mass of the composite electrode film (gram).

Supporting Information

Supporting Information is available from the Wiley Online Library or from the author.

Acknowledgements

The financial support of the Natural Sciences and Engineering Research Council of Canada (NSERC) and UQAM, NanoQAM and Professor Daniel Bélanger's laboratory members are acknowledged. The authors would like to acknowledge Profs. Sylvain Canesi and Jerome Claverie (Département de Chimie, UQAM) for their inputs for the synthesis of the materials. Nicole MacDonald from $(CM)^2$ and Marie-Claude Giguère from UQAM (Département de Chimie, UQAM) are also acknowledged for the technical assistance during SEM, EDX, and contact angle measurements.

Received: September 3, 2015
Published online: October 15, 2015

[1] P. Simon, Y. Gogotsi, B. Dunn, *Science* **2014**, *343*, 1210.
[2] F. Béguin, V. Presser, A. Balducci, E. Frackowiak, *Adv. Mater.* **2014**, *26*, 2219.
[3] F. Liu, D. Xue, *Mater. Res. Innovations* **2015**, *19*, 7.
[4] M.-S. Balogun, W. Qiu, W. Wang, P. Fang, X. Lu, Y. Tong, *J. Mater. Chem. A* **2015**, *3*, 1364.
[5] A. Laheäär, P. Przygocki, Q. Abbas, F. Béguin, *Electrochem. Commun.* **2015**, *21*, 60.
[6] B. Savage, R. Shuttleworth, N. Schofield, in *7th IET Int. Conf. Power Electron. Mach. Drives, PEMD 2014,* Institution of Engineering and Technology, London, UK **2014**, p.11204.
[7] M. Conte, A. Genovese, F. Ortenzi, F. Vellucci, *J. Appl. Electrochem.* **2014**, *44*, 523.
[8] H. D. Yoo, E. Markevich, G. Salitra, D. Sharon, D. Aurbach, *Mater. Today* **2014**, *17*, 110.
[9] D. Cericola, R. Kötz, *Electrochim. Acta* **2012**, *72*, 1.
[10] E. Karden, S. Ploumen, B. Fricke, T. Miller, K. Snyder, *J. Power Sources* **2007**, *168*, 2.
[11] H. Budde-Meiwes, J. Drillkens, B. Lunz, J. Muennix, S. Rothgang, J. Kowal, D. U. Sauer, *Proc. Inst. Mech. Eng., Part D* **2013**, *227*, 761.
[12] N. Pentyala, R. K. Guduru, P. S. Mohanty, *Electrochim. Acta* **2011**, *56*, 9851.
[13] Q. Chen, Y. Wang, T. Zhang, W. Yin, J. Yang, X. Wang, *Electrochim. Acta* **2012**, *83*, 65.
[14] L. Xiong, Y. Xu, T. Tao, J. B. Goodenough, *J. Power Sources* **2012**, *199*, 214.
[15] C. Qing, Y. Bai, J. Yang, W. Zhang, *Electrochim. Acta* **2011**, *56*, 6612.
[16] S.-L. Chou, Y. Pan, J.-Z. Wang, H.-K. Liu, S.-X. Dou, *Phys. Chem. Chem. Phys.* **2014**, *16*, 20347.
[17] C.-C. Li, Y.-W. Wang, *J. Electrochem. Soc.* **2011**, *158*, A1361.

[18] B.-R. Lee, E.-S. Oh, *J. Phys. Chem. C* **2013**, *117*, 4404.
[19] J. Li, H. M. Dahn, L. J. Krause, D.-B. Le, J. R. Dahn, *J. Electrochem. Soc.* **2008**, *155*, A812.
[20] S.-L. Chou, J.-Z. Wang, H.-K. Liu, S.-X. Dou, *J. Phys. Chem. C* **2011**, *115*, 16220.
[21] S.-L. Chou, J.-Z. Wang, C. Zhong, M. M. Rahman, H.-K. Liu, S.-X. Dou, *Electrochim. Acta* **2009**, *54*, 7519.
[22] J. Li, D.-B. Le, P. P. Ferguson, J. R. Dahn, *Electrochim. Acta* **2010**, *55*, 2991.
[23] B. Koo, H. Kim, Y. Cho, K. T. Lee, N.-S. Choi, J. Cho, *Angew. Chem. Int. Ed.* **2012**, *51*, 8762.
[24] N. S. Hochgatterer, M. R. Schweiger, S. Koller, P. R. Raimann, T. Wöhrle, C. Wurm, M. Winter, *Electrochem. Solid-State Lett.* **2008**, *11*, A76.
[25] U. Kasavajjula, C. Wang, A. J. Appleby, *J. Power Sources* **2007**, *163*, 1003.
[26] K. A. Hirasawa, K. Nishioka, T. Sato, S. Yamaguchi, S. Mori, *J. Power Sources* **1997**, *69*, 97.
[27] M. Armand, J.-M. Tarascon, *Nature* **2008**, *451*, 652.
[28] J. Chong, S. Xun, H. Zheng, X. Song, G. Liu, P. Ridgway, J. Q. Wang, V. S. Battaglia, *J. Power Sources* **2011**, *196*, 7707.
[29] L. Gong, M. H. T. Nguyen, E.-S. Oh, *Electrochem. Commun.* **2013**, *29*, 45.
[30] J. Xu, S.-L. Chou, Q. Gu, H.-K. Liu, S.-X. Dou, *J. Power Sources* **2013**, *225*, 172.
[31] I. Kovalenko, B. Zdyrko, A. Magasinski, B. Hertzberg, Z. Milicev, R. Burtovyy, I. Luzinov, G. Yushin, *Science* **2011**, *334*, 75.
[32] A. Magasinski, B. Zdyrko, I. Kovalenko, B. Hertzberg, R. Burtovyy, C. F. Huebner, T. F. Fuller, I. Luzinov, G. Yushin, *ACS Appl. Mater. Interfaces* **2010**, *2*, 3004.
[33] C. Erk, T. Brezesinski, H. Sommer, R. Schneider, J. Janek, *ACS Appl. Mater. Interfaces* **2013**, *5*, 7299.
[34] N. Delaporte, A. Perea, R. Amin, K. Zaghib, D. Bélanger, *J. Power Sources* **2015**, *280*, 246.
[35] A. Gambou-Bosca, D. Bélanger, *J. Mater. Chem. A* **2014**, *2*, 6463.
[36] Q. Abbas, D. Pajak, E. Fr ckowiak, F. Béguin, *Electrochim. Acta* **2014**, *140*, 132.
[37] S. Komaba, K. Shimomura, N. Yabuuchi, T. Ozeki, H. Yui, K. Konno, *J. Phys. Chem. C* **2011**, *115*, 13487.
[38] S. Komaba, T. Ozeki, N. Yabuuchi, K. Shimomura, *Electrochemistry* **2011**, *79*, 6.
[39] J.-P. Yen, C.-M. Lee, T.-L. Wu, H.-C. Wu, C.-Y. Su, N.-L. Wu, J.-L. Hong, *ECS Electrochem. Lett.* **2012**, *1*, A80.
[40] Z. Zhang, T. Zeng, Y. Lai, M. Jia, J. Li, *J. Power Sources* **2014**, *247*, 1.
[41] S. F. Lux, F. Schappacher, A. Balducci, S. Passerini, M. Winter, *J. Electrochem. Soc.* **2010**, *157*, A320.
[42] K.-T. Lee, C.-B. Tsai, W.-H. Ho, N.-L. Wu, *Electrochem. Commun.* **2010**, *12*, 886.
[43] J. Chong, S. Xun, H. Zheng, X. Song, G. Liu, P. Ridgway, J. Q. Wang, V. S. Battaglia, *J. Power Sources* **2011**, *196*, 7707.
[44] Z. P. Cai, Y. Liang, W. S. Li, L. D. Xing, Y. H. Liao, *J. Power Sources* **2009**, *189*, 547.
[45] S. Zhang, T. Jow, *J. Power Sources* **2002**, *109*, 422.
[46] S. Komaba, T. Ozeki, K. Okushi, *J. Power Sources* **2009**, *189*, 197.
[47] S. Komaba, K. Okushi, T. Ozeki, H. Yui, Y. Katayama, T. Miura, T. Saito, H. Groult, *Electrochem. Solid-State Lett.* **2009**, *12*, A107.
[48] A. Le Comte, T. Brousse, D. Bélanger, *Electrochim. Acta* **2014**, *137*, 447.
[49] G. Pognon, C. Cougnon, D. Mayilukila, D. Bélanger, *ACS Appl. Mater. Interfaces* **2012**, *4*, 3788.
[50] G. Pognon, T. Brousse, L. Demarconnay, D. Bélanger, *J. Power Sources* **2011**, *196*, 4117.
[51] M. Toupin, D. Bélanger, *Langmuir* **2008**, *24*, 1910.
[52] T. Matrab, M. M. Chehimi, C. Perruchot, A. Adenier, A. Guillez, M. Save, B. Charleux, E. Cabet-Deliry, J. Pinson, *Langmuir* **2005**, *21*, 4686.
[53] C. Combellas, F. Kanoufi, J. Pinson, F. I. Podvorica, *Langmuir* **2005**, *21*, 280.
[54] C. Combellas, M. Delamar, F. Kanoufi, J. Pinson, F. I. Podvorica, *Chem. Mater.* **2005**, *17*, 3968.
[55] M. M. Chehimi, A. Lamouri, M. Picot, J. Pinson, *J. Mater. Chem. C* **2014**, *2*, 356.
[56] J. A. Belmont, C. Bureau, M. M. Chehimi, S. Gam-Derouich, J. Pinson, *Aryl Diazonium Salts*, Wiley-VCH, Weinheim, Germany **2012**.
[57] S. Mahouche-Chergui, S. Gam-Derouich, C. Mangeney, M. M. Chehimi, *Chem. Soc. Rev.* **2011**, *40*, 4143.
[58] T. Liu, R. Casado-Portilla, J. Belmont, K. Matyjaszewski, *J. Polym. Sci., Part A: Polym. Chem.* **2005**, *43*, 4695.
[59] K. Matyjaszewski, *Macromolecules* **2012**, *45*, 4015.
[60] A. Le Comte, D. Chhin, A. Gagnon, R. Retoux, T. Brousse, D. Belanger, *J. Mater. Chem. A* **2015**, *3*, 6146.
[61] G. Pognon, T. Brousse, D. Bélanger, *Carbon* **2011**, *49*, 1340.
[62] A. C. Ferrari, S. E. Rodil, J. Robertson, *Phys. Rev. B: Condens. Matter Mater. Phys.* **2003**, *67*, 1553061.
[63] S. A. S. T. W. Graham Solomons, C. B. Fryhle, *Organic Chemistry*, Wiley, New York, NY, USA **2014**.
[64] K. Balasubramanian, M. Burghard, *Small* **2005**, *1*, 180.
[65] P. Simon, Y. Gogotsi, *Nat. Mater.* **2008**, *7*, 845.
[66] D. Pech, D. Guay, T. Brousse, D. Bélanger, *Electrochem. Solid-State Lett.* **2008**, *11*, A202.
[67] O. Barbieri, M. Hahn, A. Herzog, R. Kötz, *Carbon* **2005**, *43*, 1303.